

NANOSTRUCTURES FROM PHASE SEPARATED POLYMERS

Michael. R. Bockstaller and Edwin L. Thomas*

Massachusetts Institute of Technology, 77 Massachusetts Ave., Cambridge, 02139 MA

*) email: ELT@MIT.EDU

KEYWORDS

polymer, block copolymer, phase separation, self-assembly, nanostructures, liquid crystal, photonic crystal, thin film, lithography

The field of polymer-based materials continues its enormous growth covering a wide range of products from disposable coffee cups to car bumpers to biomedical devices. The increased emphasis on enhancement of properties via materials with structures of components engineered on the nanoscale has opened up many new opportunities. For example, blending different polymers while retaining their individual properties in the composite is an effective way of engineering new nano- and microstructural materials from a limited palette of commodity polymers. At present five major reasons for the technological importance of polymer multicomponent systems can be identified: (1) improvements in material performance via synergistic interactions (e.g. temperature resistance, modulus, adhesion); (2) realizing desired processing conditions (e.g. melt viscosity, softening point, solvent resistance); (3) recycling industrial or municipal scrap polymers; (4) adjusting product composition to customer specifications by mixing of different batches and (5) dilution of high performance polymers for cost reduction.

Despite their great industrial relevance, there exists no formally accepted nomenclature for multicomponent polymer systems. A possible classification scheme is provided in Scheme 1. Understanding and controlling the mechanisms of phase separation and nanostructure formation in polymer systems allows one to tailor the performance of these materials to a manifold of applications. For example, co-continuous blends of high- and low-melting point polymers where the low-melting point component is the majority component facilitate to dramatically increase thermal and mechanical properties such as toughness, stress at break or high-temperature creep resistance while retaining ease of processability. Recent research suggests possible future applications of multicomponent polymer systems that are more far-reaching. Nanostructures based on block copolymer-homopolymer blends are currently studied as a platform for photonic materials with possible use in integrated optics or in thin films as non-lithographic route towards

controlled patterning of 100 nm feature sizes. The future technological impact of the latter type of applications will crucially depend on the ability to control structure formation on multiple lengthscales by strategic design of chemical groups as well as integrating synthetic design with specific processing pathways that increase the likelihood of attaining a targeted structure.

This article reviews polymer phase behavior and nanostructure formation beginning with a discussion of molecular architecture, equilibrium thermodynamics and phase separation dynamics. The second part describes recent achievements to control the structure formation processes over macroscopic dimensions. The interplay of relevant balancing forces in self-organization processes is discussed aiming to give the reader some intuition about how molecular details and processing conditions can be used in order to control structure formation.

In the third part, new research areas will be presented in which polymer based nanostructures are likely to have major technological impact. Throughout, examples will focus on synthetic polymers that are either of high industrial interest or suitably represent characteristics of a broad range of macromolecules but leaving out the complex structure formation processes found in natural biopolymers.

MOLECULAR ARCHITECTURE AND PHASE DIAGRAM

The term *polymer* means “many units” and designates a large molecule made up of smaller repeating units the number of which determines the degree of polymerization N . Other basic quantities characterizing a polymer chain are the molecular weight $M=Nm$, with m being the molecular weight of a single repeat unit, and its radius of gyration R_G which scales as $N^{1/2}$ for

flexible chains in their melt state. As a rule of thumb, molecular weights of common-type flexible polymers of $M \sim 10^5$ g/mol correspond to an effective size of the polymer chain of $R_G \sim 10$ nm. The inherent length scale in the nanometer range renders polymer materials naturally attractive for nanoengineering purposes. Depending on the synthetic procedure, the repeating unit of a linear polymer may comprise a single identifiable precursor such as in poly(styrene) or might be composed of the residues of several smaller molecules as in poly(hexamethylene-adipamide) (Nylon-6,6). Table 1 shows the chemical structures of a small selection of polymers relevant to this article. Next to the linear chain architecture, synthetic strategies have been developed to also obtain well-defined star- or branched molecular structures. For a detailed discussion of methods for polymer synthesis the reader is referred to [1, 2]. A small subset of the wealth of architectures is shown in Scheme 2. Depending on molecular architecture, degree of polymerization and temperature, the physical state of polymeric materials can vary between viscous liquid, glassy, semi-crystalline or liquid crystalline. Crystallization processes, which require a highly regular stereochemistry of the polymer, and the associated hierarchy of structures are beyond the scope of this article and will only briefly be mentioned.

Homopolymer Blends

The equilibrium phase behavior of a mixture of two linear polymers A and B was first derived by Flory [3] and Huggins [4]. According to Flory-Huggins theory, the change in free energy upon mixing ΔG_m for a binary polymer blend is given by

$$\frac{\Delta G_m}{k_B T} = \frac{\phi_A}{N_A} \ln \phi_A + \frac{\phi_B}{N_B} \ln \phi_B + \phi_A \phi_B \chi \quad (1)$$

with k_B denoting the Boltzmann constant, T the temperature, $N_{A/B}$ the degree of polymerization

(the number of mers of A and of B), $\phi_{A/B}$ the volume fraction of polymer A and B and χ the Flory-Huggins segment-segment interaction parameter. Since large chains assume fewer mixed configurational states, the entropic contribution (first two terms in Eq.1) decreases with increasing molecular weight of the polymers. The phase behavior of binary polymer blends is then largely determined by the value of χ that is fixed by the particular choice of the repeating units of polymer A and B. χ parameters can often be expressed as a linear function of $1/T$, i. e. $\chi(T)=\alpha+\beta/T$; values for α and β have been tabulated for a variety of monomers [5]. Given a binary polymer mixture, the phase behavior can be predicted by calculation of the spinodal and binodal that are given by the criteria of stability (Eq. 2) and thermodynamic equilibrium (Eq. 3), respectively.

$$\frac{\partial^2 \Delta G_m}{\partial \phi_A^2} = 0 \quad (2)$$

$$\frac{\partial \Delta G_m(\phi_A)^{phase1}}{\partial \phi_A} = \frac{\partial \Delta G_m(\phi_A)^{phase2}}{\partial \phi_A} \quad (3)$$

The binodal and spinodal curves meet in the critical point that is given for a symmetric polymer blend with equal molecular volumes ($N_A v_A = N_B v_B$, v_i denoting the volume of monomer i) by $\phi_c = 1/2$ and $\chi_c = 2/N$. A typical phase diagram for a binary mixture of symmetric linear homopolymers is shown in Figure 1. Depending on the sign and temperature dependence of χ , different types of phase behavior can be distinguished, the most important are referred to as: UCST (upper critical solution temperature, mixing upon heating) which is found for positive χ and $d\chi/d(1/T) > 0$ as well as LCST (lower critical solution temperature, mixing upon cooling) which is found for negative χ and $d\chi/d(1/T) < 0$. In a few experimental systems, closed-loop behavior has been observed, i.e. low temperature LCST and high temperature UCST [6]. Table 2

shows a list of some homopolymers that are frequently found in industrial applications and their mixing behavior.

Mechanisms of phase separation in homopolymer blends

There are two major mechanisms of phase separation that have been identified and that occur in different parts of the phase diagram as shown in Figure 1: nucleation and growth (NG) and spinodal decomposition (SD). NG occurs in the metastable region of the phase diagram (the area between binodal and spinodal) and is characterized by the following steps: a) initial formation of spherical fragments of the more stable phase (requires activation barrier) b) growth of nuclei by first diffusion of material from the supersaturated continuum followed by droplet-droplet coalescence and Ostwald-ripening. SD, which is the commonly observed mechanism for phase separation in homopolymer blends, occurs in the unstable region of the phase diagram and is characterized by initial small- amplitude composition fluctuations that increase with time and result in interconnected phase morphologies at intermediate stages of phase separation. Co-continuous polymer blends have been the subject of intense research since they generally exhibit superior mechanical properties. Co-continuous interconnected morphologies are commonly induced either by arresting SD or by mechanical mixing of polymer mixtures. Such systems often suffer the problem that they tend to move towards the equilibrium macrophase-separated structure. Blending of homopolymers in the presence of appropriately chosen graft copolymers has been shown to be a versatile alternative to mechanical mixing, facilitating the stabilization of co-continuous blends by increasing the thermodynamic stability and flexibility of the interface [7]. Figure 2 shows the microstructure of a poly(ethylene)/poly(amide) co-continuous blend and the associated enhancement of elastic and tensile properties. Note that the elastic modulus

increases by order of magnitudes in the case of the co-continuous blend with regard to its phase separated counterpart.

Block Copolymers

Block copolymers consist of two distinct polymer chains that are covalently linked together to form a chain. The large variety of block configurations that can be constructed using modern synthetic methods can be classified based on the number of chemically distinct blocks as well as linear versus branched connectivity of the blocks within a copolymer as indicated in Scheme 3. Since structure formation processes of most of these systems are still under discussion, this article will focus on the current understanding of the simplest and most studied system – linear amorphous diblock copolymers. For excellent review articles in this field we refer the reader to [8, 9, 10].

Because block copolymers are single component systems, they cannot macrophase-separate in the melt like a pair of linear homopolymers does. Instead, block copolymers segregate on a local scale. The decrease of A-B segment contacts by local segregation is often referred to as microphase-separation. The enthalpy gain obtained by the local segregation process is counterbalanced by an associated loss in system entropy that results from the localization of the block joints at the intermaterial dividing surface (IMDS) and the necessary stretching of the polymer chains away from the IMDS in order to maintain uniform density. Since the entropic contribution can be shown to scale as N^{-1} with $N=N_A+N_B$, it is again the product χN that dictates the microphase separation process. Three different limiting regimes exist for diblock copolymer melts: a) the disordered state with unperturbed Gaussian chain statistics ($R_G \sim N^{1/2}$) which is found for $\chi N \ll 1$, b) the ordered state in the weak segregation limit ($\chi N \sim 10$) with sinusoidal

composition fluctuations representing a periodic microstructure and c) the ordered state in the strong segregation limit ($\chi N \gg 10$) where strong repulsive forces between segments of A and B result in sharp interfaces separating nearly-pure A and B domains with pronounced stretching of the block chains ($R_G \sim N^{2/3}$). Below the order-disorder transition temperature, enthalpic effects become more influential and the block copolymer microphase separates. The product χN and the compositional parameter $f = N_A / (N_A + N_B)$ determine one of seven phases that represent free-energy minima for the ensemble of molecular configurations. The following sequence of phases has been observed for PS-PI diblocks: $f_{PS} < 0.17$, body centered cubic (BCC); $0.17 < f_{PS} < 0.28$, hexagonal; $0.28 < f_{PS} < 0.34$, bicontinuous (double gyroid); $0.34 < f_{PS} < 0.62$, lamellar; $0.62 < f_{PS} < 0.66$, inverse double gyroid; $0.66 < f_{PS} < 0.77$ inverse hexagonal; $f_{PS} > 0.77$, inverse BCC. Depending on the packing frustration self-consistent field calculations also suggested the formation of a double diamond and a perforated lamellar structure between the well established lamellar and cylinder phases, but these microdomain geometries are considered to be only metastable and will not be discussed here. A phase diagram along with a schematic of the different periodic microstructures found as a function of χN and f for a typical diblock copolymer are shown in Figure 3. Figure 4 demonstrates the observation of the above mentioned morphologies via electron micrographs of PS-PI diblock copolymers.

Block copolymer – homopolymer blends

A natural continuation of the research mentioned above is the study of block copolymer/homopolymer blends. Structure formation in blends of homopolymers and block copolymers is determined by the interplay of macrophase-separation of the homopolymer and the microphase-separation of the block copolymer. Which effect predominates depends on the

relative lengths of the respective polymers and on the composition of the blend. In binary blends, low-molecular weight homopolymer is solubilized within a microphase-separated block copolymer structure at low concentrations. Increasing the molecular weight of the homopolymer such that it approaches that of the block copolymer leads to an increasing tendency for segregation of the homopolymer to the center of the domain. If the molecular weight of the homopolymer exceeds the one of the block copolymer, macrophase- separation tends to predominate [11].

Binary block copolymer blends

Binary block copolymer blends offer another route towards nanoscale structures. Binary blends of triblock (ABC) and diblock (ac) copolymers, with the upper and lower case characters distinguishing the chemical composition and molecular weight of the respective blocks, were extensively studied due to their potential to microphase-separate into *non-centrosymmetrical* morphologies. These nanostructures are of high technological interest, as the absence of centrosymmetry implies macroscopic polarization that is associated with many useful properties like piezo- and pyroelectricity and second-order non-linear optical activity. Theoretical studies on the formation of non- centrosymmetric morphologies were performed for the case of lamellar structure and suggest that non-centrosymmetrical morphologies require sufficient asymmetry between the Aa and Cc domains. Figure 5 shows a schematic of possible lamellar morphologies in blends of ABC and ac block copolymers along with an excellent electron micrograph providing non-centrosymmetrical lamellar structure was obtained by blending a poly(styrene-b-butadiene-b-tert-butylmethacrylate) triblock copolymer with poly(styrene-b-tert-butylmethacrylate) diblock copolymer [12].

STRATEGIES FOR CONTROLLING THE SELF-ORGANIZATION PROCESSES

Mechanical behavior can be readily tuned when e.g. glassy mesostructures are formed in a rubbery matrix, and indeed, glassy-rubbery block copolymers are used for various applications as advanced engineering materials. However, the possible impact of block copolymer nanostructures that is envisioned is much more far-ranged. The emerging challenges that have to be resolved involve the extension of hierarchically ordered structures to larger length scales and the development of new processing technologies that allow to control the ordering process at various length scales. In the following sections, several approaches will be presented that address these challenges. (1) strategic design of the molecular architecture, e.g. by introducing anisotropic groups that introduce configurational constraints to the self-assembling process, (2) by exploiting the effect of external fields on the self-assembly process or (3) by using surface energetics and selective polymer-substrate interactions to guide the system to the desirable global geometries.

Techniques Involving Molecular Architecture

Structure formation in rod-coil block copolymer systems

If one block in a coil-coil block copolymer is substituted by a polymer type that exhibits highly restricted conformational freedom, a rod-coil block copolymer is obtained. The interest in rod-coil block copolymers is fueled by the extraordinary wealth of morphologies that are found in rod-coil systems, which can result in novel functional materials with intriguing optical or electronic properties. This spectrum of domain morphologies is due to the delicate interplay between liquid crystallinity of the rod block combined with the phase-separated microdomain

morphologies. Rod-coil block copolymers also provide an excellent example of *designer nanoscale materials* as the rod blocks represent active sites that can be addressed by external fields (flow, electric, magnetic) providing a means to guide the system into well-defined macroscopically ordered states. A rod-like conformation of a polymer is induced either by stepwise coupling of rigid mesogenic units to form low-molecular weight oligomeric rods or in macromolecular systems by creating a rigid polymer backbone with alternating conjugation, by steric hindrance of side groups attached to each repeating unit or by the formation of helical secondary-structures. The asymmetry in the rigidity of the respective rod vs. coil blocks significantly increases the Flory-interaction parameter χ , such that rod-coil block copolymers microphase-separate already at low weight fractions of the rod component. The hierarchical order from the nano- to the micronscale results as a consequence of the mutual repulsion of the dissimilar blocks and the packing constraints that are imposed by the connectivity as well as the tendency towards orientational ordering of the rod block.

Currently, there exists no general theoretical framework that can account for the complex phase behavior thus observed in rod-coil copolymer systems. Three examples will be provided that represent some of the new morphologies that are encountered in rod-coil block copolymer systems. For excellent review articles of this field we refer the reader to [13, 14].

Stupp et al. reported the formation of large, well-organized supramolecular structures (10^2 kD) by self-assembly of rod-coil *oligomers* consisting of an elongated mesogenic rods with volume filling fractions ranging from 0.19 to 0.36 and a coil-like poly(isoprene) part [15]. Depending on the rod filling fraction, the formation of a strip morphology ($f_{\text{rod}}=0.36$) or a hexagonal superlattice structure ($f_{\text{rod}}=0.25$) was observed. Substituting the poly(isoprene) coil block by a (styrene)₉-b-(isoprene)₉ oligomer was reported to result in the formation of mushroom-like

assemblies containing about $N=100$ rod-coil oligomers that self-organize into superlattice domains. A schematic of the proposed structure is given in Figure 6.

Chen et al. investigated the structures formed in *high-molecular* rod-coil block copolymer systems consisting of poly(hexylisocyanate) with $N=900$ as the rod block and poly(styrene) with $N=300$ as the coil block [16]. Depending on the volume fraction of rod component, the formation of three different morphologies was reported. These were explained to occur as the result of microphase separation of the blocks and crystallization of the rods during solvent evaporation. For a volume filling fraction of the rod component $f_{\text{rod}}=0.42$, the formation of a wavy lamellar structure was observed, in which the rod blocks are tilted with respect to the layer normal by about 60° . For $f_{\text{rod}}=0.73$ a novel “zigzag” morphology was observed in which the rod and coil blocks are arranged in a zigzag fashion and the rod blocks are tilted with respect to the layer normal by 45° . For even higher rod filling fractions ($f_{\text{rod}}>0.96$) an “arrowhead-like” pattern formation was observed. Figure 7 shows electron micrographs of the observed morphologies. The complexity of the structure formation process in rod-coil systems is indicated by the pronounced effect of solvent on the structures depicted in Figure 7. Well-oriented zigzag patterns were observed only when toluene was used, whereas the use of chloroform as a solvent resulted in more disordered arrangement of the zigzags. The observed difference can be understood since the quality of the solvent determines the onset of microphase separation of the blocks as well as the onset of liquid-crystallization of the rod blocks. As a consequence, rod-coil morphologies often do not represent equilibrium structures but rather kinetically trapped states. Park et al. have continued the study of microstructure formation in rod-coil block copolymers and demonstrated the formation of long-range periodic domain walls yielding a hierarchical morphology with order on multiple length scales consisting of inter-chain crystals of the rod blocks (1.5 nm), block

copolymer microdomains (55 nm) and periodic Neel domain walls ($\sim 1 \mu\text{m}$) [17]. This study is remarkable for two reasons. First, the block copolymer -- poly(3-(triethoxysilyl)propylisocyanate-b-styrene) -- employed in their study contains reactive groups as part of the isocyanate rod blocks. These entities allow the polymer to be covalently tethered to inorganic substrates after microstructure formation. Second, by directional solvent evaporation, the authors demonstrated unidirectional alignment of domain wall patterns on the centimeter lengthscale while maintaining inter-chain and microdomain ordering. A pair of atomic force micrographs of the observed hierarchical rod-coil structure are shown in Figure 8.

Effect Of Mechanical And Electric Fields

Polymeric materials can undergo dramatic changes in their structure in response to external fields. This provides opportunities to direct distinct alignments of polymeric nanostructures through processing. Polymer engineers have long exploited processing to increase properties (e.g. fiber production) through increase of crystallinity and chain orientation. For many envisioned applications of polymer-based nanostructures, it is of special importance to be able to produce functional macroscopic materials with uniform large-scale orientation. In general, self-assembly processes alone do not result in globally ordered structures but rather heterogeneous morphologies consisting of randomly oriented grains within which the domains have homogeneous alignment. The possibility to induce global order in block copolymer microstructures by flow field alignment was pioneered by Keller et al. in extruded polymer materials and a variety of other flow methods have been developed, such as roll-casting and extensional flow [18, 19, 20]. Kornfield et al. studied the influence of oscillatory shear on the

alignment of lamellar morphology forming block copolymers by in-situ rheo-optical methods that allow monitoring the alignment of the lamellae as a function of applied shear rate and amplitude [19]. It was argued that with increasing shear rate three different frequency regimes can be distinguished for layered microstructured block copolymers in which the polymer domains have dissimilar viscoelastic properties. Two characteristic frequencies that determine the effect of oscillatory shear on the alignment of lamellar samples were identified: a lower frequency limit ω_d that is associated with the lifetime of fluctuations on a layered structure and a higher frequency limit ω_c that reflects the dynamics of conformational distortions of single polymer chains. It was found that oscillatory strain shearing induces parallel alignment with respect to the shear direction for $\omega < \omega_d$, perpendicular alignment for $\omega_d < \omega < \omega_c$ and parallel alignment for $\omega_c < \omega$.

For cylindrical microdomain forming coil-coil block copolymers subjected to steady or oscillatory shear, parallel orientation, i.e. the cylinder axes are aligned along the flow direction, was found to be the usual orientational state. However, by anchoring liquid crystalline side groups to a coil-coil block copolymer Osuji et al. could demonstrate that the strong interaction of the mesogens with the applied flow field can force the cylindrical microdomains to align *transverse* to the flow direction [21]. In their study of the effect of oscillatory mechanical shear on the microstructure formation of a poly(styrene)-poly(isoprene) block copolymer in which each isoprene block was functionalized with a mesogenic group, the authors concluded that the invariant homogeneous anchoring of the mesogens with respect to the IMDS results in the transverse cylindrical orientation under shear. A schematic of the proposed structural model of perpendicular smectic layers and transverse cylindrical microdomains is given in Figure 9.

Amundson et al. [22] presented a detailed mechanistic study of the effect of electrical fields on

the structure evolution in lamellar block copolymer systems. By applying electrical fields of 1.8 MV/m to a symmetric PS-PMMA diblock copolymer while heating the polymer above glass transition temperature, a significant increase in orientation of the lamellae along the electric field direction could be observed. The ordering effect of the electric field could be explained by the orientational dependence of the systems free-energy in the presence of the external field. The situation is similar to the effect of an oscillatory shear-field when $\omega < \omega_d$. The external field raises the free-energy associated with lamellar compression or splay and hence causes movement and annihilation of defect walls and disclination lines. A schematic of the defect movement along with electron micrographs of the films with and without electric field alignment is shown in Figure 10. Recently, Russel et al. applied a similar procedure to align cylindrical PS-PMMA block copolymers using electric field strengths of 40 MV/m [23].

Thin Film Morphologies

Whereas bulk morphologies of microphase-separated block copolymers are often typified by grains of ordered domains that are randomly oriented with respect to each other, thin films can sometimes exhibit highly ordered domains. This orientation can be understood as a direct result of the surface and interfacial energy minimization. The possible applications of block copolymer thin films have been widely recognized and constitute a very active current field of research. An excellent introduction to the field is the recent review article by Fasolka et al. [24]. Of the various microdomain types, the most investigated is the lamellar. Most theoretical work regarding the physics of thin film morphology was done for the case of symmetrical boundary conditions that is realized, e.g. when the film is located in between two identical substrates. It was found that for films with thickness greater the lamellar thickness, $t > L$, the lamellae orient

parallel to the substrate surface. As a result of the surface substrate boundary conditions the most energetically compatible block is expressed at each of the surfaces. Depending on which block wets the respective surface, one distinguishes between symmetric (same block wets each surface) and anti-symmetric (different blocks wet the two surfaces) wetting. The equilibrium conditions for stability of symmetric films are then given as $t=nL$, with n being an integer, and $t=(n+1/2)L$ for anti-symmetric wetting. It was proposed that the entropic penalty that is imposed on chains when surface-parallel lamellae are constrained to film thicknesses incommensurate with integer multiples of L can induce the perpendicular lamellar orientation if the entropic penalty exceeds the enthalpic gain from preferential wetting. A summary of possible thin film morphologies is given in Figure 11.

Although the assumption of symmetric boundary conditions simplifies the analysis, many practical thin film situations exhibit asymmetric boundary conditions, e.g. supported film systems. In supported film systems, the polymer-substrate interfacial energy of a given type of monomer can differ from its surface energy by an order of magnitude. The presence of asymmetric boundary conditions can therefore result in new morphological trends not found in the symmetric case, e.g. the formation of hybrid structures involving parallel as well as perpendicular alignment. At the time of writing no theoretical model has been developed that could accurately account for many of the experimental observations. This is in part due to the finite roughness and deformability of most surfaces on the molecular scale that represents a major problem in the application of the theoretical models mentioned above to real supported films.

Epitaxial crystallization of block copolymer thin films

Epitaxy denotes the oriented overgrowth of one crystalline material upon the surface of another. In general, this process requires an approximate agreement in lattice spacings of the two components. Epitaxy is a traditional method of material science used to control registration and orientation. Block copolymers which contain one crystallizable block are of great interest since the crystallization provides an additional driving force for the microphase-separation. The resulting morphology is the result of the interplay between segregation and crystallization process and is therefore process-path dependent, resulting in new opportunities to control the structure formation process by directing the crystallization process. Epitaxial methods were shown to be particularly interesting in controlling the orientation of microphase separated block copolymer domains over large areas. De Rosa et al. recognized that due to the crystallographic matching of poly(ethylene) and benzoic acid crystals, the poly(ethylene) blocks of a semicrystalline poly(ethylene-b-ethylenepropylene-b-ethylene) triblock copolymer can be epitaxially crystallized onto crystals of benzoic acid thereby directing the microphase separation process [25]. Electron micrographs depicting the microstructure of the block copolymer thin film with and without epitaxial direction are shown in Figure 12. Epitaxial control over the microphase separation process continues to attract a lot of attention as it opens a new dimension to the control of nanostructure formation: crystal orientation on the 1-10 nm length scale as well as microstructure orientation on the 10-100 nm lengthscale.

TRENDS IN EXPLOITING POLYMER-BASED NANOSTRUCTURES

Recent advances in understanding the formation of nanostructures based on self-assembled microphase separated block copolymers and the external parameters that afford global ordering

of these structures has resulted in applications that capitalize on the specific structural characteristics rather than on a volume averaged behavior. Microphase separated block copolymers have been studied extensively as an alternative approach to conventional lithographic techniques to produce highly ordered nanostructures with possible applications such as a high-density magnetic recording device or a photonic band-gap material. In the following we present some examples of the new directions in this area of research.

Block Copolymers As Photonic Band Gap Materials

Since block copolymers self-assemble into periodic one-, two- or three dimensional equilibrium structures, optical effects like photonic band gaps can be obtained when the molecular weight of the block copolymer is high enough such that the domain spacing is of the order of the wavelength of light (typically $M \sim 10^6$ g/mol). Photonic band gaps denote frequency regions in which light of certain polarization and propagation direction cannot propagate through the material [26]. Since the synthesis and processing of high molecular weight polymers is delicate, the first observation of a self-assembled polymer-based photonic material was not published until 1999 [27]. Various techniques have been developed in order to solve the eminent problem of the inherently low dielectric contrast between typical polymers. Methods such as selective deposition of high index nanocrystals within the polymer scaffold [28] or selective etching of one of the domains [29] can raise the dielectric contrast. It could be shown that even for high molecular weight copolymers the double gyroid microdomain morphology can be obtained, indicating pathways to 3 dimensional photonic crystals that combine a full photonic band gap with the advantageous mechanical properties of polymeric materials and the ease of self-assembly. Figure 13b shows a scanning electron micrograph of a double gyroid obtained from high

molecular weight PS-PI after selective etching of the PI matrix using UV/ozone [29].

Block Copolymer Lithography

The typical length scale of microphase separation, 10-100 nm, is particularly interesting as it provides a versatile alternative to conventional photolithographic techniques for surface structuring. Possible applications for regular texturing of a surface at the 10 nm lengthscale are the fabrication of high storage magnetic recording media, DNA electrophoresis membranes or micro-optical elements. Of particular interest is the combination of the controlled structure formation on the nanometer length scale with the distinct chemical nature of the respective blocks. Jaeger et al. demonstrated the selective decoration of the PS domains of a cylindrical microstructure forming PS-PMMA diblock copolymer by evaporation of gold on top of the spin-casted polymer thin film [30]. The dense packing of gold nanocrystals on the PS domains allowed for the formation of a regular pattern of conducting nanowires 50 nm in width which are of great interest as interconnects, gratings or for biosensor applications. A schematic of the described structure formation process along with electron micrographs of the resulting structures is shown in Figure 14. Block copolymer lithography has also been studied as possible alternative to conventional lithographic techniques for the fabrication of high-density magnetic storage media. For example, Cheng et al. demonstrated that single-domain ferromagnetic cobalt dots can be fabricated using self-assembled block copolymer lithography [31]. In their study, the authors took advantage from the significantly different etching rates of organic-inorganic block copolymers when exposed to a reactive ion beam, allowing the selective etching of one component from the microstructure while converting the inorganic containing block to a ceramic. A thin film of spherical microdomain morphology forming poly(styrene-b-

ferrocenyldimethylsilane) PS-PFS block copolymer was cast on a layered cobalt-tungsten-silica substrate and the PFS domains used as a mask for subsequent reactive ion etching. A schematic of the procedure as well as a scanning electron micrograph of the obtained nanodot arrays is shown in Figure 15.

Inorganic-Organic Mesostructures From Block Copolymer Phases

At present, great attention is being paid to the preparation of complex inorganic-organic hybrid materials with long-range order that could find possible applications in catalysis, membrane and separation technology. Two major synthetic approaches can be distinguished: (1) the in-situ synthesis of inorganic particles within a block copolymer domain that has been loaded with a suitable precursor reagent and (2) the simultaneous self-assembly of the block copolymer in the presence of ex-situ synthesized nanoparticles that are surface-tailored in order to allow preferential sequestration within a target domain. Whereas the first approach facilitates higher volume filling fractions of the inorganic material, the second approach allows better control of the structural characteristics of the sequestered component. Micropatterned solid particles in a block copolymer matrix were produced by Bootongkong et al. in a nanoreactor scheme, in which the hydrophilic domain of a poly(styrene-*b*-acrylic acid) block copolymer is pre-loaded with a metal salt, that is reduced in a second reaction step [32]. The procedure is outlined in Figure 16. The authors demonstrated that the block copolymer nanoreactor scheme might be applied to a wide variety of metal (Pd, Cu, Au, Ag) as well as semiconductor (PbS) nanocrystals. Whereas the block copolymer nanoreactor scheme results in the formation of discrete or interconnected nanocrystals dispersed within the respective block copolymer domain, Templin et al. demonstrated that by swelling of the poly(ethylene oxide) domain of a poly(ethylene oxide-*b*-

isoprene) block copolymer with an inorganic precursor followed by hydrolysis and calcination, continuous inorganic nanorelief structures can be obtained [33]. The authors also described the formation of the “Plumber’s Nightmare” morphology for the hybrid material, which is an uncommon bicontinuous morphology for block copolymers and which was explained by subtle differences in the phase behavior of hybrid versus neat block copolymer structures. In contrast to the above mentioned in-situ approaches, ex-situ methodologies become advantageous when precise control of the structural features of the inorganic component becomes relevant to the desired function of the hybrid material or the geometrical characteristics of the inorganic component cannot be obtained through in-situ synthesis. For example, Ha et al. studied the incorporation of “two-dimensional” clay sheets into lamellar PS-PI block copolymer microstructures [34]. The authors demonstrated that by decorating the mineral’s surface with poly(styrene), individual clay sheets can be preferentially sequestered within the polystyrene domain of the block copolymer. The resulting nanocomposite materials exhibit highly anisotropic mechanical and permeability properties. An electron micrograph of the nanocomposite material revealing single-layer clay sheets sequestered within the poly(styrene) domains is shown in Figure 17. The development of surface decoration techniques that allow for molecular level dispersion of the inorganic component within the polymer matrix represents a major advancement in the field since the inclusion of single-sheet (exfoliated) mineral layers permits to downscale the amount of inorganic component by an order of magnitude (only 2 wt% inorganic is needed) while providing the advantageous material properties.

The control of the composites’ architecture on the nanometer scale is of special importance for future research in this area as it facilitates to dramatically decrease the switching speed in these materials which is diffusion limited, scaling as the square of the feature size. At present, research

focus is on the development of next-generation actuator materials that capitalize from both, the mechanical and optical characteristics of the sequestered component as well as the rapid dynamic response to external stimulus that results from the architectural control on the molecular level.

ACKNOWLEDGEMENTS

This material is based upon work supported by, or in part by, the Alexander von Humboldt Foundation (Feodor-Lynen program) as well as the U.S. Army Research Laboratory and the U.S. Army Research Office under Contract DAAD-19-02-0002. We thank Dr. J.-W. Park, A. M. Urbas and Y.-H. Ha for their contribution of electron and atomic force micrographs to this work.

REFERENCES

- [1] Hiemenz, P. C. *Polymer chemistry: the basic concepts*. Marcel Dekker, New York, (1984).
- [2] Hadjichristidis, N.; Pitsikalis, M; Pispas S.; Iatrou, H. Polymers with Complex Architecture by Living Anionic Polymerization. *Chem. Rev.* **2001**, *101*, 3747-3792.
- [3] Flory, P. J. J. Thermodynamics of high polymer solutions. *Chem. Phys.* **1941**, *9*, 660.
- [4] Huggins, M. L. J. Solutions of long chain compounds. *Chem. Phys.* **1941**, *9*, 440.
- [5] Balsara, N. P.; Fetters, L. J.; Hadjichristidis, N. Thermodynamic interactions in model polyolefin blends obtained by small-angle neutron scattering. *Macromolecules* **1992**, *25*(23), 6137.
- [6] Ryu, D. Y.; Jeong, U.; Kim, J. K.; Russel, T. P. Closed-loop phase behavior in block copolymers. *Nature Materials* **2002**, *1*, 114-117.
- [7] Pernot, H.; Baumert, M.; Court F.; Leibler L. Design and properties of co-continuous nanostructured polymers by reactive blending. *Nature Materials* **2002**, *1*, 54-58.
- [8] Bates, F. S. Polymer-polymer phase behavior. *Science* **1991**, *251*, 898-905.
- [9] Bates, F. S.; Fredrickson G. H. Block copolymer thermodynamics. *Annu. Rev. Phys.* **1990**, 525-557.
- [10] Hamley, I. W. *The physics of block copolymers*. Oxford University Press, New York, (1998).
- [11] Winey, K. I.; Thomas, E. L.; Fetters, L. Swelling a lamellar diblock copolymer with homopolymer-influences of homopolymer concentration and molecular weight. *Macromolecules* **1991**, *24*(23), 6182-6188.
- [12] Goldacker, T.; Abetz, V.; Stadler, R.; Eruhimovich, I.; Leibler, L. Non-centrosymmetric

superlattices in block copolymer blends. *Nature* **1999**, *398*, 137-139.

[13] Lee, M.; Cho, B.-K.; Zin, W.-C. Supramolecular structures from rod-coil block copolymers. *Chem. Rev.* **2001**, *101*, 3869-3892.

[14] Klok, H.-A.; Lecommandoux, S. Supramolecular materials via block copolymer self-assembly. *Adv. Mater* **2001**, *13*(16), 1217-1229.

[15] Stupp, S. I.; LeBonheur, V.; Walker, K.; Li L. S.; Huggins K. E.; Keser M.; Amstutz, A. Supramolecular materials: self-organized nanostructures. *Science* **1997**, *276*, 384-389.

[16] Chen, J. T.; Thomas, E. L.; Ober, C. K.; Mao, G. P. Self-assembled smectic phases in rod-coil block copolymers. *Science* **1996**, *276*, 343-346.

[17] Park, J.W.; Thomas, E. L. Multiple ordering transitions: hierarchical self-assembly of rod-coil block copolymers. *Nature Materials* **2002**, *in press*.

[18] Honeker, C. C.; Thomas, E. L. Perpendicular deformation of a near-single-crystal triblock copolymer with a cylindrical morphology. *Macromolecules* **2000**, *33*(25), 9407-9417.

[19] Chen, Z.-R.; Kornfield, J. A.; Smith, S. D.; Grothaus J. T.; Sattkowski, M. M. Pathways to macroscale order in nanostructured block copolymers. *Science* **1997**, *277*, 1248-1253.

[20] Keller, A.; Pedemonte, E.; Willmouth, F. M. Macro lattice from segregated amorphous phases of a three block copolymer. *Colloid. Polym. Sci.* **1970**, *238*, 385-389.

[21] Osuji, C.; Zhang, Y.; Mao, G.; Ober, C. K.; Thomas, E. L. Transverse cylindrical microdomain orientation in a LC diblock copolymer under oscillatory shear. *Macromolecules* **1999**, *32*, 7703-7706.

[22] Amundson, K.; Helfand, E.; Quan, X.; Smith, S. D. Alignment of block copolymer microstructures. *Macromolecules* **1994**, *27*(22), 6559-6570.

[23] Thurn-Albrecht, T.; Schotter, J.; Kastle, G. A.; Emley, N.; Shibauchi, T.; Krusin-Elbaum, L;

- Guarini, K.; Black, C. T.; Tuominen M. T.; Russel T. P. Ultrahigh-density nanowire arrays grown in self-assembled diblock copolymer templates. *Science* **2000**, *290*, 2126-2129.
- [24] Fasolka M. J.; Mayes, A. M. Block copolymer thin films: physics and applications. *Annu. Rev. Mater. Res.* **2001**, *31*, 323-355.
- [25] De Rosa, C.; Park, C.; Thomas, E. L.; Lotz, B. Microdomain patterns from directional eutectic solidification and epitaxy. *Nature* **2000**, *405*, 433-437.
- [26] Joannopoulos, J. D.; Meade, R. D.; Winn, J. N. *Photonic Crystals*. Princeton University Press, New Jersey, (1995).
- [27] Fink, Y.; Urbas, A. M.; Bawendi, M. G.; Joannopoulos, J. D.; Thomas, E. L. Block copolymers as photonic bandgap materials. *Journal of Lightwave Technology* **1999**, *17*(11), 1963-1969.
- [28] Bockstaller, M. R.; Kolb, R.; Thomas, E. L. Metallodielectric photonic crystals based on diblock copolymers. *Adv. Mater.* **2001**, *13*(23), 1783-1786.
- [29] Urbas, A. M.; Maldovan, M.; Thomas, E. L. Bicontinuous Cubic Photonic Crystal in a Block Copolymer System . *Adv. Mater.* **2002**, *in press*.
- [30] Lopes, W. A.; Jaeger, H. M. Hierarchical self-assembly of metal nanostructures on diblock copolymer scaffolds. *Nature* **2001**, *414*, 735-738.
- [31] Cheng, J. Y.; Ross, C.; Chan, V. Z.-H.; Thomas, E. L.; Lammertink, R. G. H.; Vansco, G. J. Formation of cobalt magnetic dot array via block copolymer lithography. *Adv. Mater.* **2001**, *13*(15), 1174-1178.
- [32] Boontongkong, Y.; Cohen, R. E. Cavitated block copolymer micellar thin films: lateral arrays of open nanoreactors. *Macromolecules* **2002**, *35*(9), 3647-3652.
- [33] Templin, M.; Franck, A.; Du Chesne, A.; Leist, H.; Zhang, Y.; Ulrich, R.; Schaedler, V.; Wiesner, U. Organically modified aluminosilicate mesostructures from block copolymer phases.

Science **1997**, 278, 1795-1798.

[34] Ha, Y. H.; Thomas, E. L. Deformation behavior of roll-cast layered silicate/triblock copolymer nanocomposites. *Macromolecules* **2002**, 35(11), 4419-4428.

FIGURE CAPTIONS

Table 1. Structure and nomenclature of selected polymers.

Table 2. Mixing behavior of selected homopolymer blends.

Scheme 1. Multicomponent polymer system classification scheme. The types of polymer blends relevant to this text are marked in black.

Scheme 2. Selection of homopolymer architectures.

Scheme 3. Selection of di- and multiblock copolymer architectures.

Figure 1. a) Phase diagram of a symmetric homopolymer blend ($N_A=N_B$). Shaded area indicates metastable region. b) Schematic of the mechanism of phase separation in the metastable (nucleation and growth, NG) and instable (spinodal decomposition, SD) region of the phase diagram.

Figure 2. Transmission electron micrographs of a) co-continuous nanostructured blend (80/20 ratio poly(ethylene)/Nylon-6,6); b) phase separated blend. c) and d) show increase of elastic modulus and stress-strain properties for co-continuous phase formation. Triangles: co-continuous (80/20), squares: micellar blend (80/20), diamonds: macrophase separated blend, circles: poly(ethylene). (Reprinted by permission from Nature Materials [8] copyright (2002) Macmillan Publishers Ltd.).

Figure 3. Phase diagram of a symmetric block copolymer ($N_A=N_B$). L: lamellar phase, C: cylindrical phase, G: Gyroid phase, S: spherical phase (cubic body centered).

Figure 4. Transmission electron micrographs of a) lamellar; b) hexagonal cylindrical viewing direction along cylinder axis, inset: viewing direction perpendicular to cylinder axis; c) gyroid (view direction along (110)) and d) BCC spherical phase of poly(styrene-b-isoprene) copolymer (along (100)). For all micrographs, the isoprene block was stained with Osmiumtetroxide to enhance contrast.

Figure 5. a) diagram of the possible lamellar morphologies of ABC/ac block copolymer blends. 1: macrophase separation, 2: random sequence, 3: centrosymmetric sequence, 4: non-centrosymmetric sequence. b) Transmission electron micrograph of the non-centrosymmetric blend. (Reprinted by permission from Nature [13] copyright (1999) Macmillan Publishers Ltd.).

Figure 6. Transmission electron micrograph revealing superlattice of regularly shaped aggregates. Inset: Suggested mushroom-like morphology of the aggregate. (Abstracted from [16] Copyright[2001] American Association for the Advancement of Science.)

Figure 7. Transmission electron micrographs of the morphologies of the PHIC-PS rod-coil block copolymer: wavy-lamellar ($f_{\text{PHIC}}=0.42$), zig-zag ($f_{\text{PHIC}}=0.89$) and bilayer arrowhead ($f_{\text{PHIC}}=0.96$). The dark regions correspond to PS (stained with Rutheniumoxide). (Abstracted from [17] Copyright[2001] American Association for the Advancement of Science).

Figure 8. Tapping mode atomic force micrographs of the hierarchical structure formation of PS-PIHC thin films after casting on silica substrate. The insets show Fourier transformed images.

Figure 9. Schematic structural model of the transverse alignment of cylindrical microdomains and smectic layers. Flow is along x- and vorticity is along y-direction. The model represents a compromise structure in which cylinders are transverse and smectic layers are perpendicular but the boundary condition for the mesogens are maintained homogeneous. (adapted from [22] with permission of the American Chemical Society).

Figure 10. a) Movement of the disclination lines and wall defects occurring by glide and climb of edge dislocations and creation of pores. 1: disclination lines approach by perforation of layer; 2: focal conic loop forms island that grows by climb motion along the disclination loop; 3: through combination of climb and glide motion an edge dislocation propagates along a wall defect. b) transmission electron micrographs of PS-PMMA perpendicular to field direction and c) parallel to field direction. (Adapted from [23] with permission of the American Chemical Society).

Figure 11. Diblock copolymer thin film morphologies as a function of boundary conditions. A block is gray, B-block is black. L_0 : film thickness, FL: symmetric surface-parallel full lamellae, AFL: anti-symmetric surface-parallel lamellae, AHY: anti-symmetric hybrid structure, HL: half-lamellae, HY: symmetric hybrid structure, PL: surface-perpendicular lamellae. (Adopted from [24] with permission of Annual Reviews, copyright 2002).

Figure 12. Transmission electron micrographs of a) solvent-cast and b) directionally solidified/epitaxially crystallized PS-PE copolymer. PE domains form pseudo-hexagonal lattice of perpendicular oriented cylinders. The styrene blocks have been stained with Rutheniumtetroxide for contrast enhancement. The inset in b) shows magnified region demonstrating the non-circular shape of the PS-PE interface resulting from the 15% smaller domain spacing of benzoic acid in

b- direction.

Figure 13. a) Schematic model of the double Gyroid morphology showing two interpenetrating networks (here: PS) embedded in the matrix material (here: air). Scanning electron micrograph of a free-standing interconnected PS network obtained from a high molecular weight Double Gyroid PS-PI block copolymer after selective UV/ozone etching of the PI domain.

Figure 14. a) Metal nanochain and nanowire formation after vapor-deposition of Au onto a thin film of cylindrical PS-PMMA block copolymer and annealing for one minute at 180 °C under Ar atmosphere. Au highly selective decorates the PS domain. b) Magnification of a) demonstrating individual nanocrystal array formation. (Reprinted by permission from Nature Materials [30] copyright (2001) Macmillan Publishers Ltd.).

Figure 15. Tilted scanning electron micrograph showing Co-nanodot arrays obtained after complete etching of the PS-PFS block copolymer. (Adopted from...).

Figure 16. a) Schematic of the nanoreactor approach. 1: thin film cast of spherical PS-PAA; 2: selective swelling of PAA spheres with metal precursor; 3: formation of metal nanocrystals by reduction of metal precursor. b) Transmission electron micrograph of thin film demonstrating hexagonal array of Ag nanodots within PS matrix.

Figure 17. Transmission electron micrograph of exfoliated clay-PS-PI nanocomposite. Individual PS-decorated clay sheets are sequestered within PS layers. Inset: schematic of the composite structure.

TABLE 1

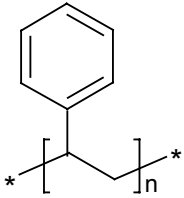
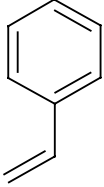
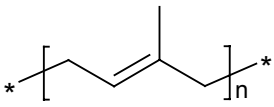
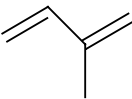
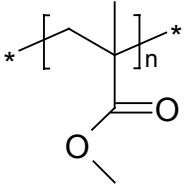
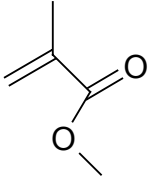
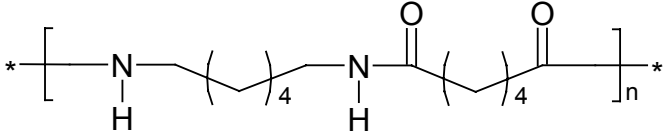
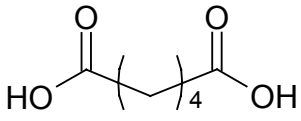
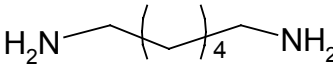
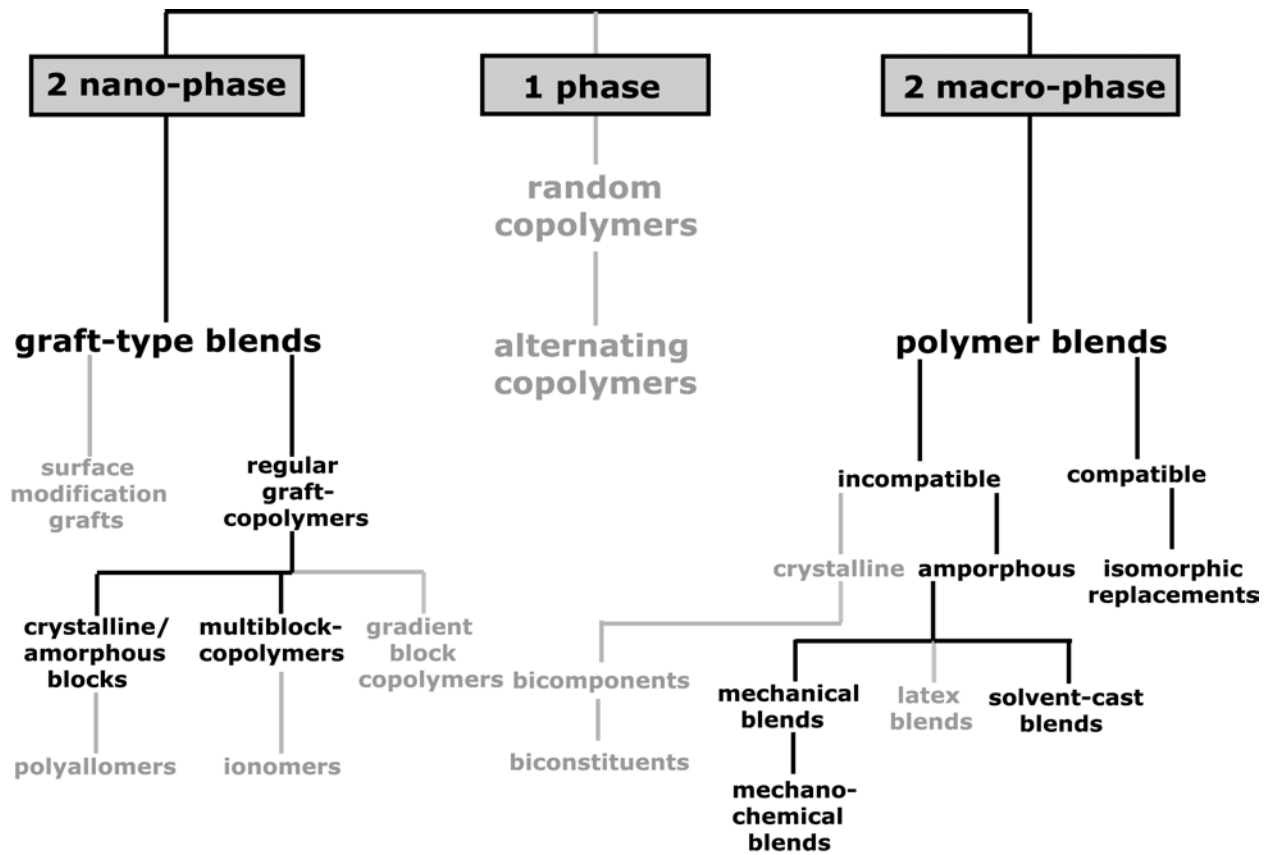
Structure	Monomer	Nomenclature (Abbreviation)
		Poly(styrene) (PS)
		Poly(isoprene) (PI)
		Poly(methylmethacrylate) (PMMA)
	 	Poly(hexamethylene adipamid) (Nylon-6,6)

TABLE 2

Polymer 1	Polymer 2	Miscibility
poly(styrene)	poly(butadiene)	NO
poly(styrene)	poly(methyl methacrylate)	NO
poly(styrene)	poly(dimethyl siloxane)	NO
Nylon-6,6	poly(ethylene-propylene)	NO
poly(propylene)	poly(ethylene)	NO
poly(styrene)	poly(vinyl methylether)	YES
poly(styrene)	poly(dimethyl phenyleneoxide)	YES
poly(ethylene oxide)	poly(acrylic acid)	YES
poly(vinylchloride)	poly(butylene terephthalate)	YES
poly(methyl methacrylate)	poly(vinylidene fluoride)	YES

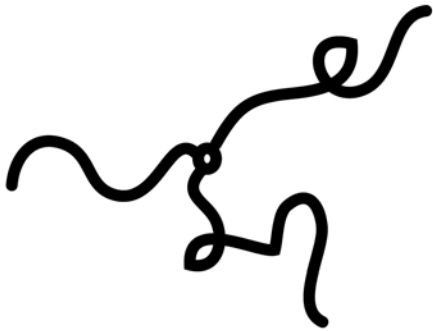
SCHEME 1



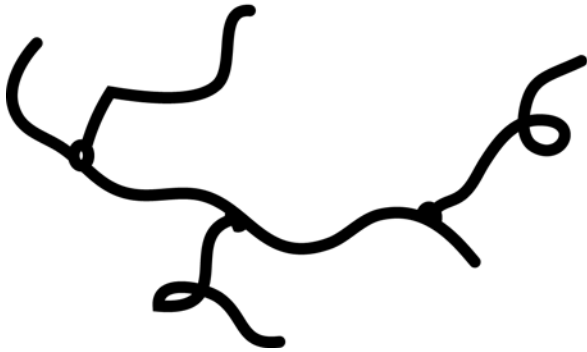
SCHEME 2



linear



star



branched

SCHEME 3

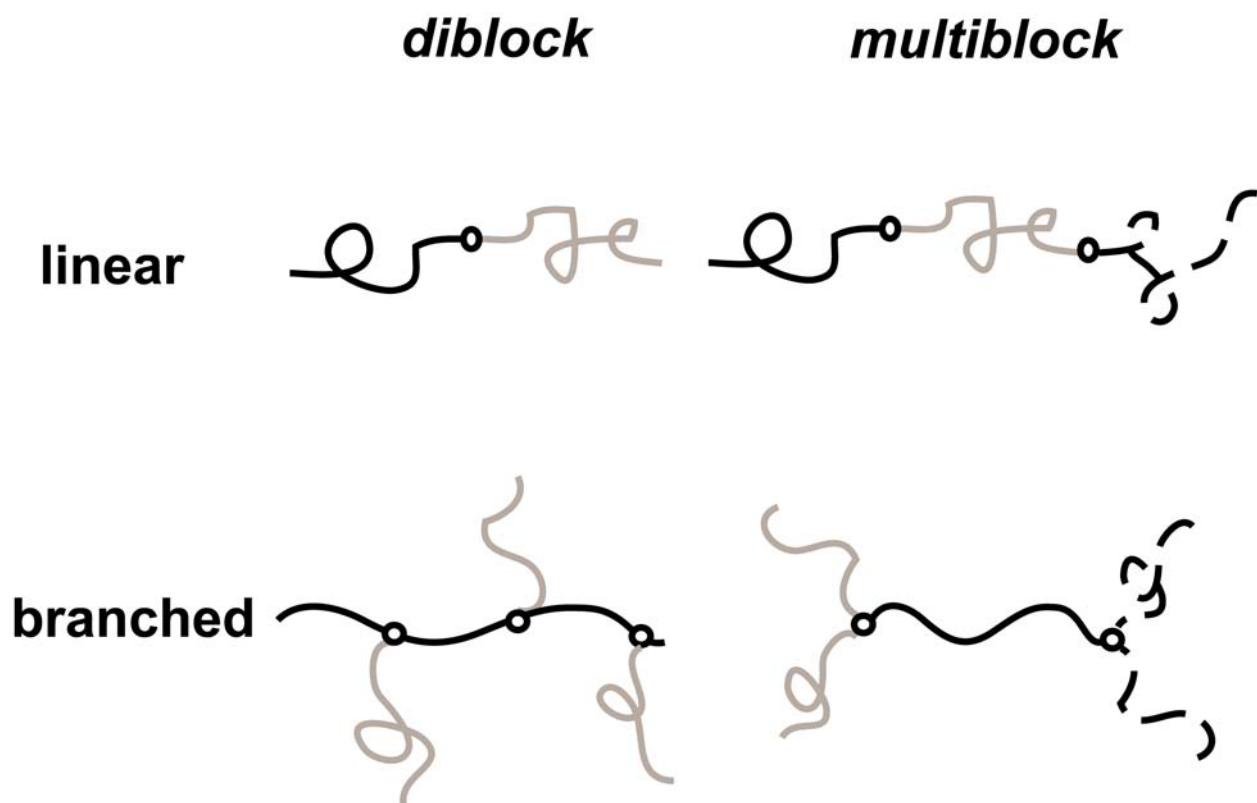
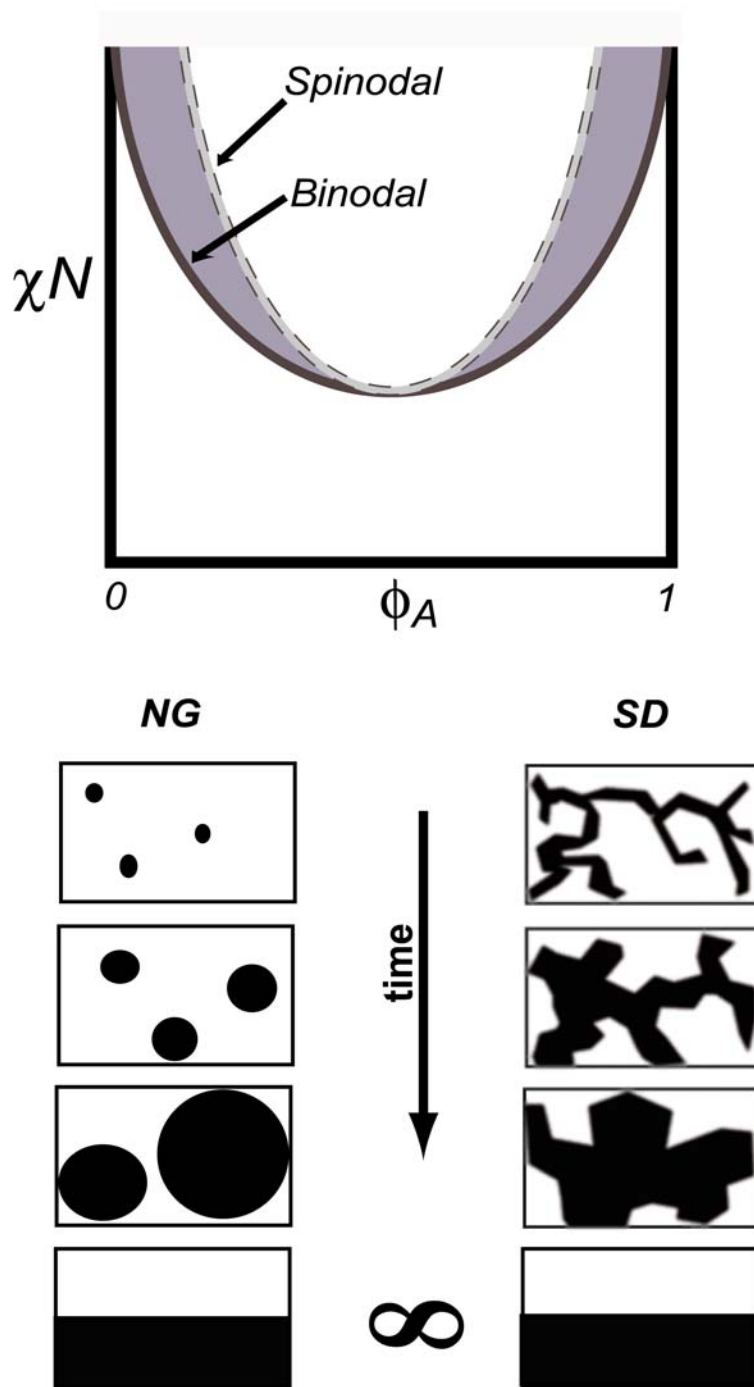
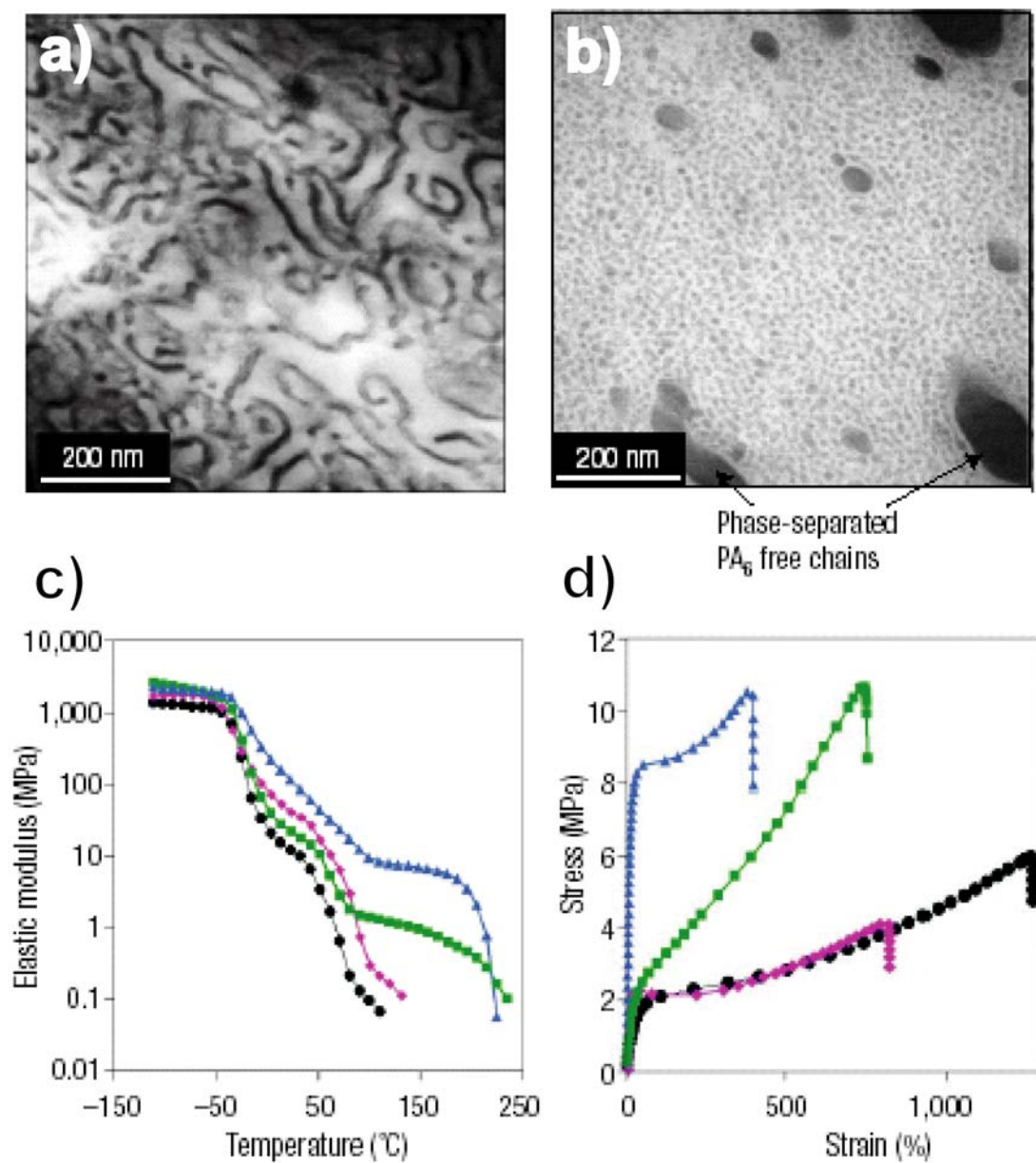


FIGURE 1



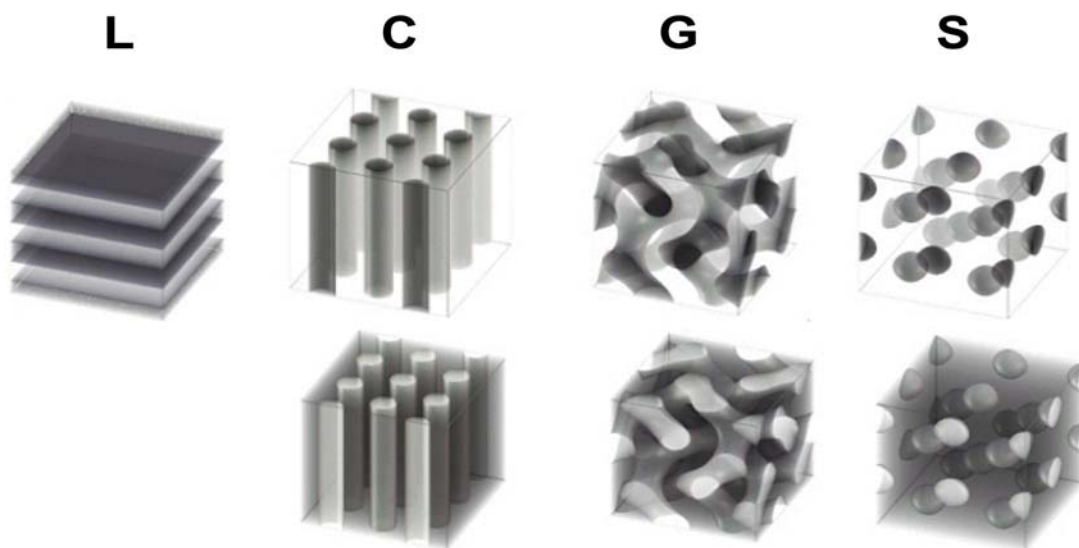
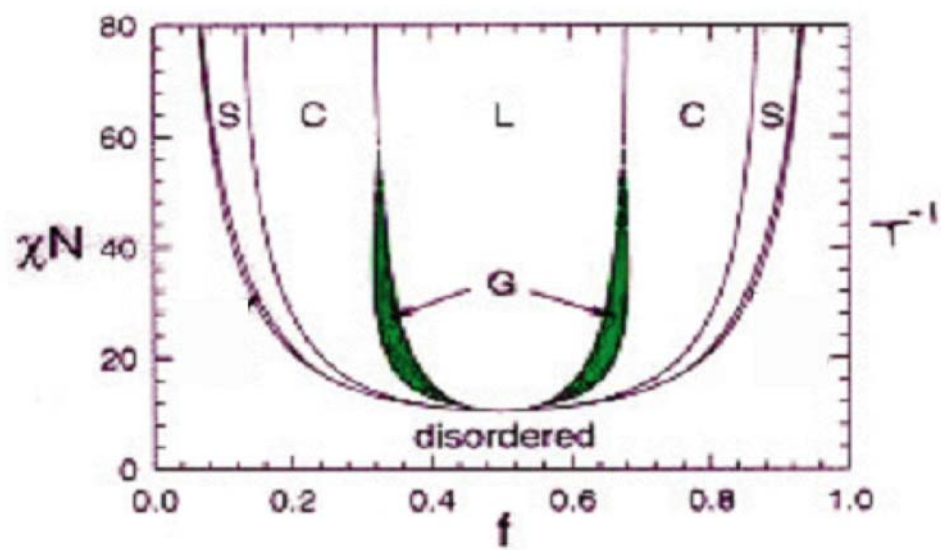
Bockstaller et al.

FIGURE 2



Bockstaller et al.

FIGURE 3



Bockstaller et al.

FIGURE 4

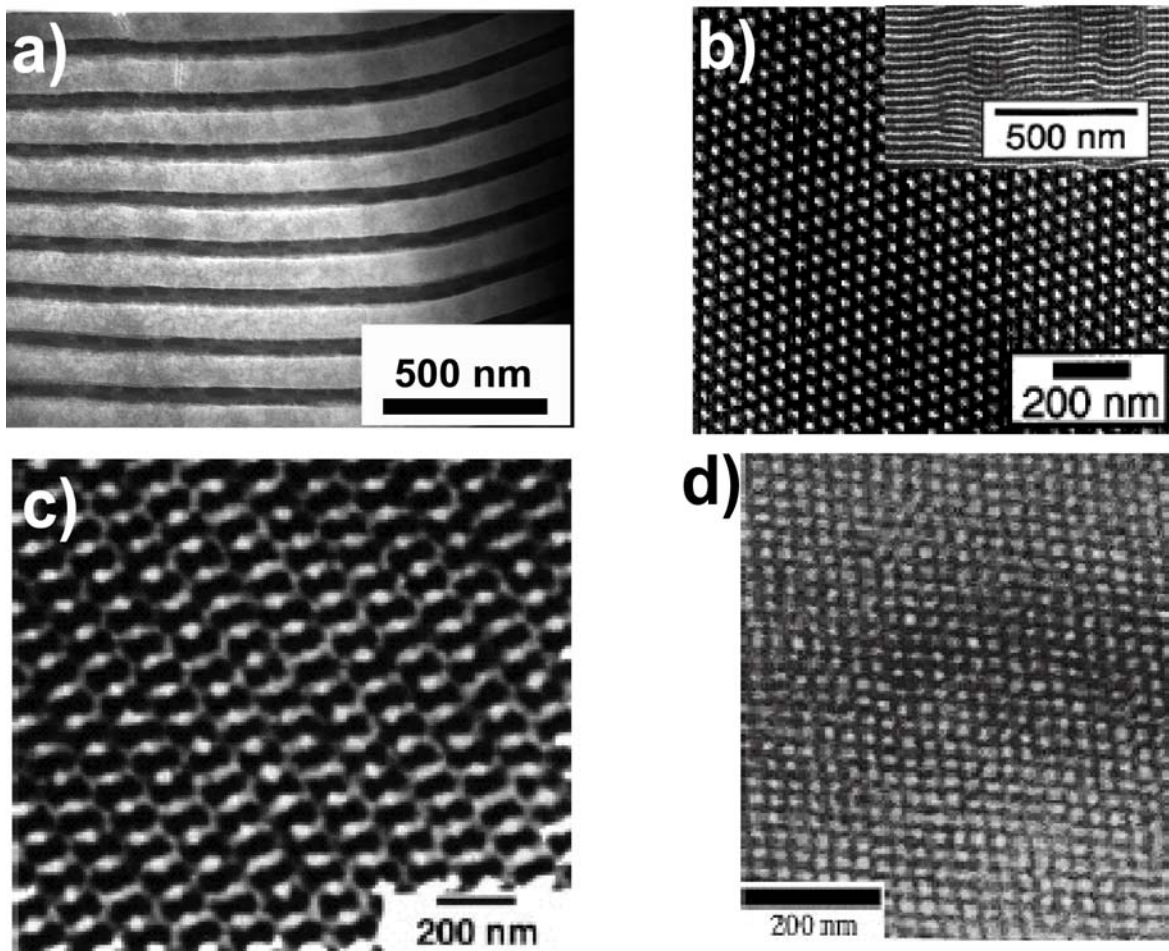
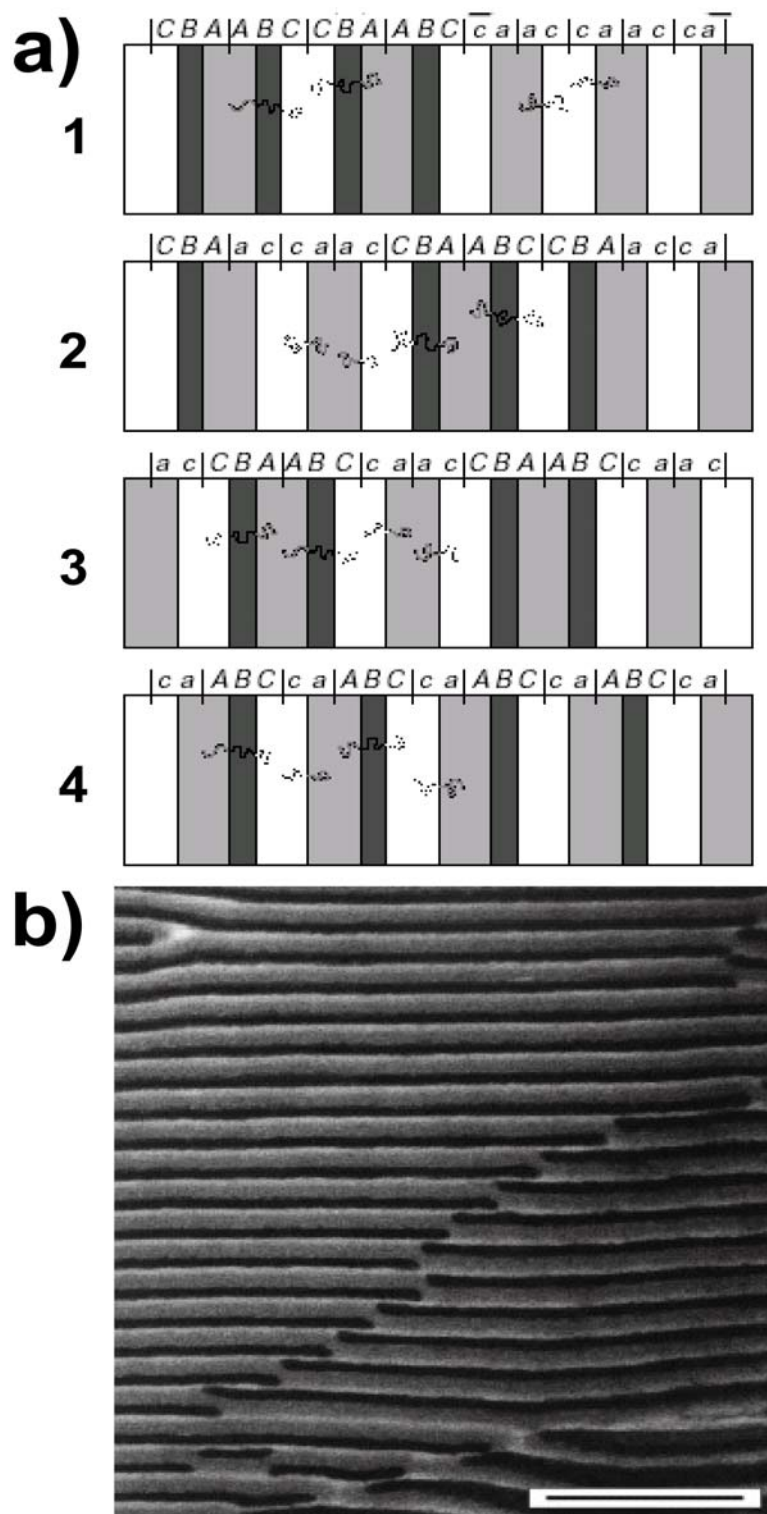


FIGURE 5



Bockstaller et al.

FIGURE 7

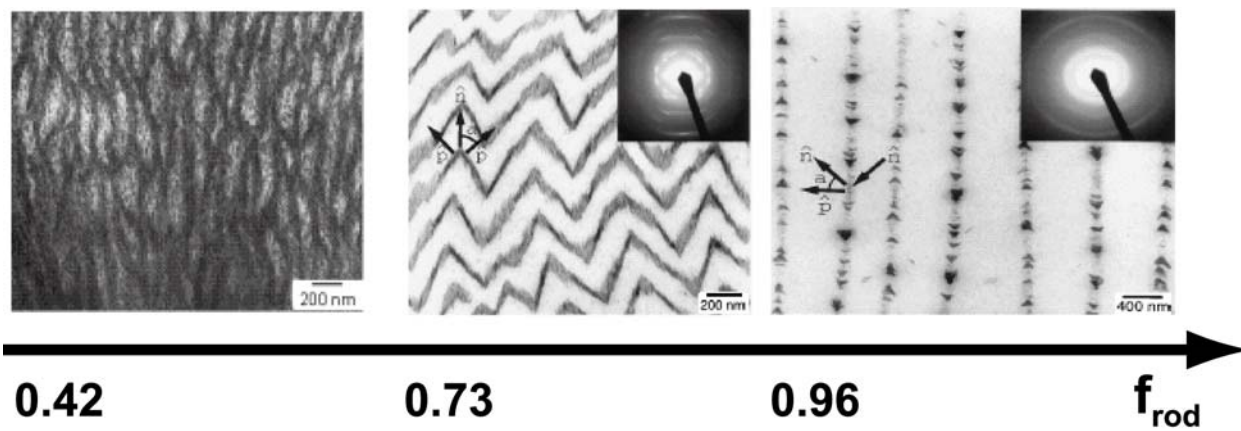


FIGURE 8

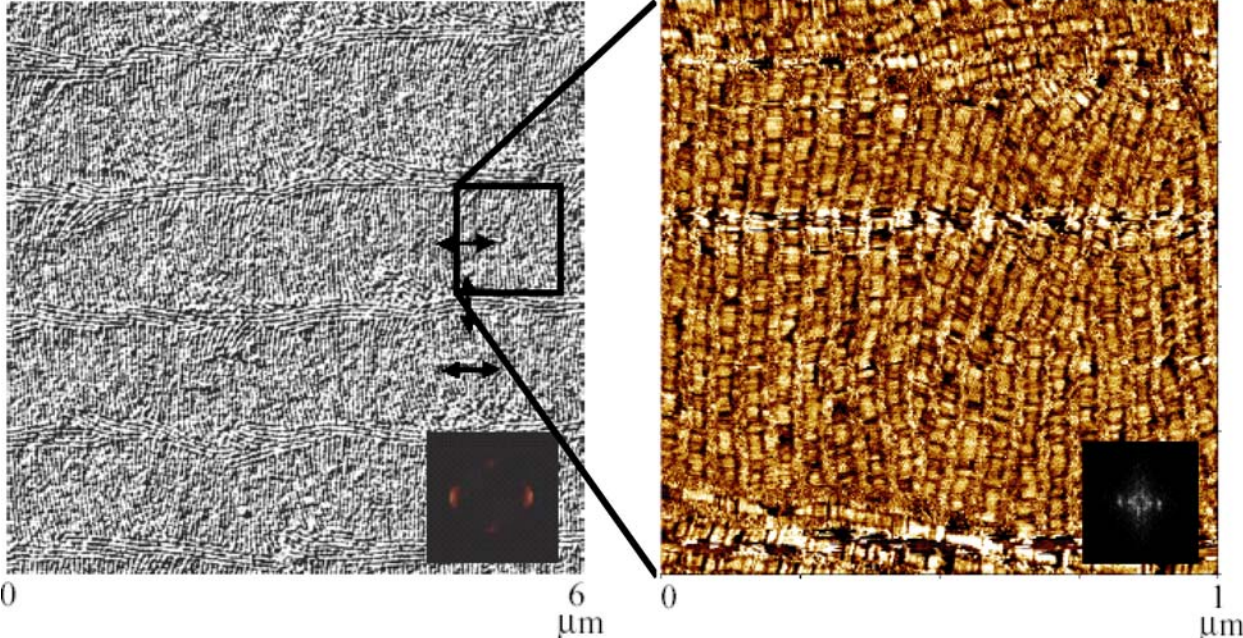


FIGURE 9

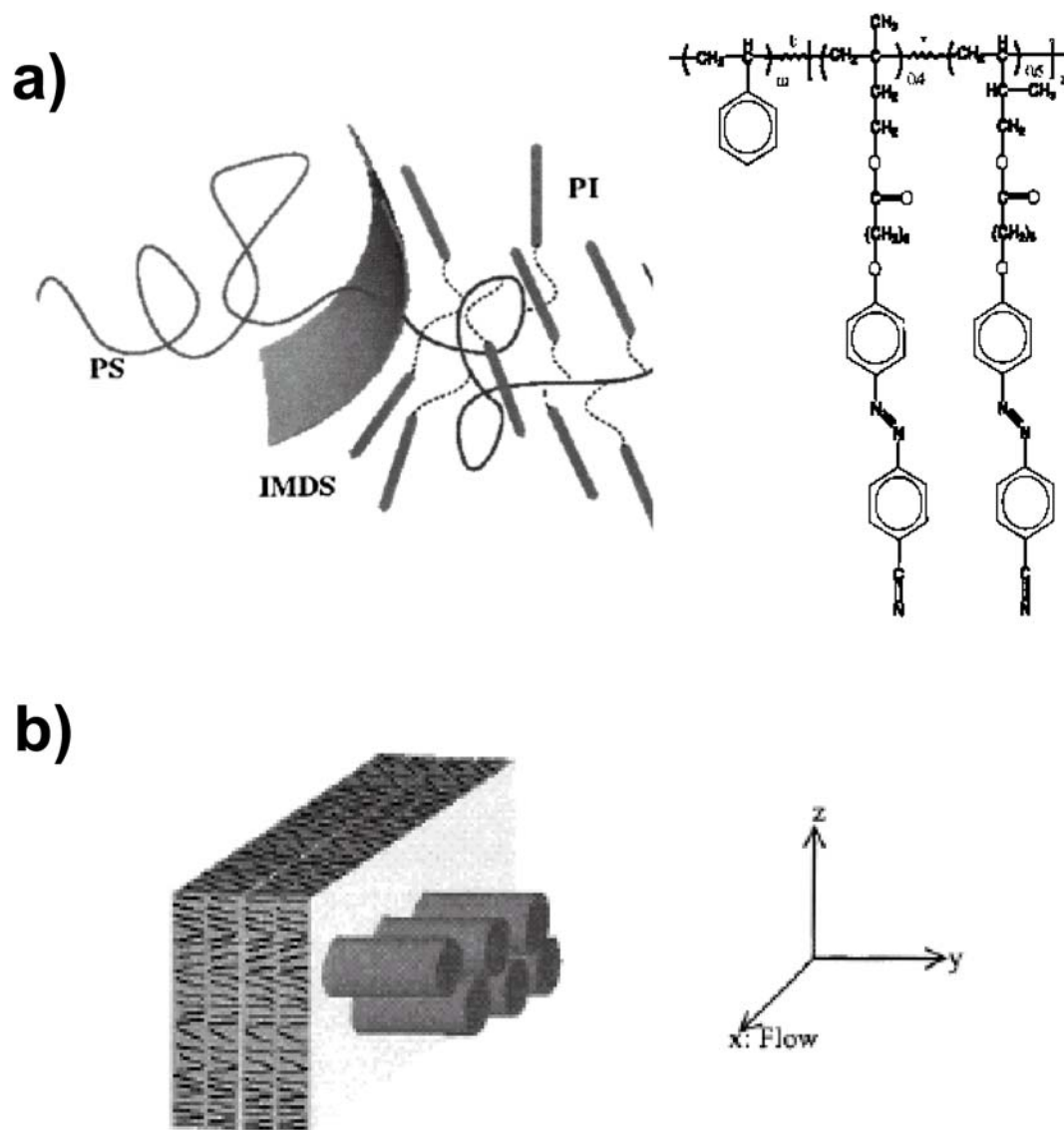
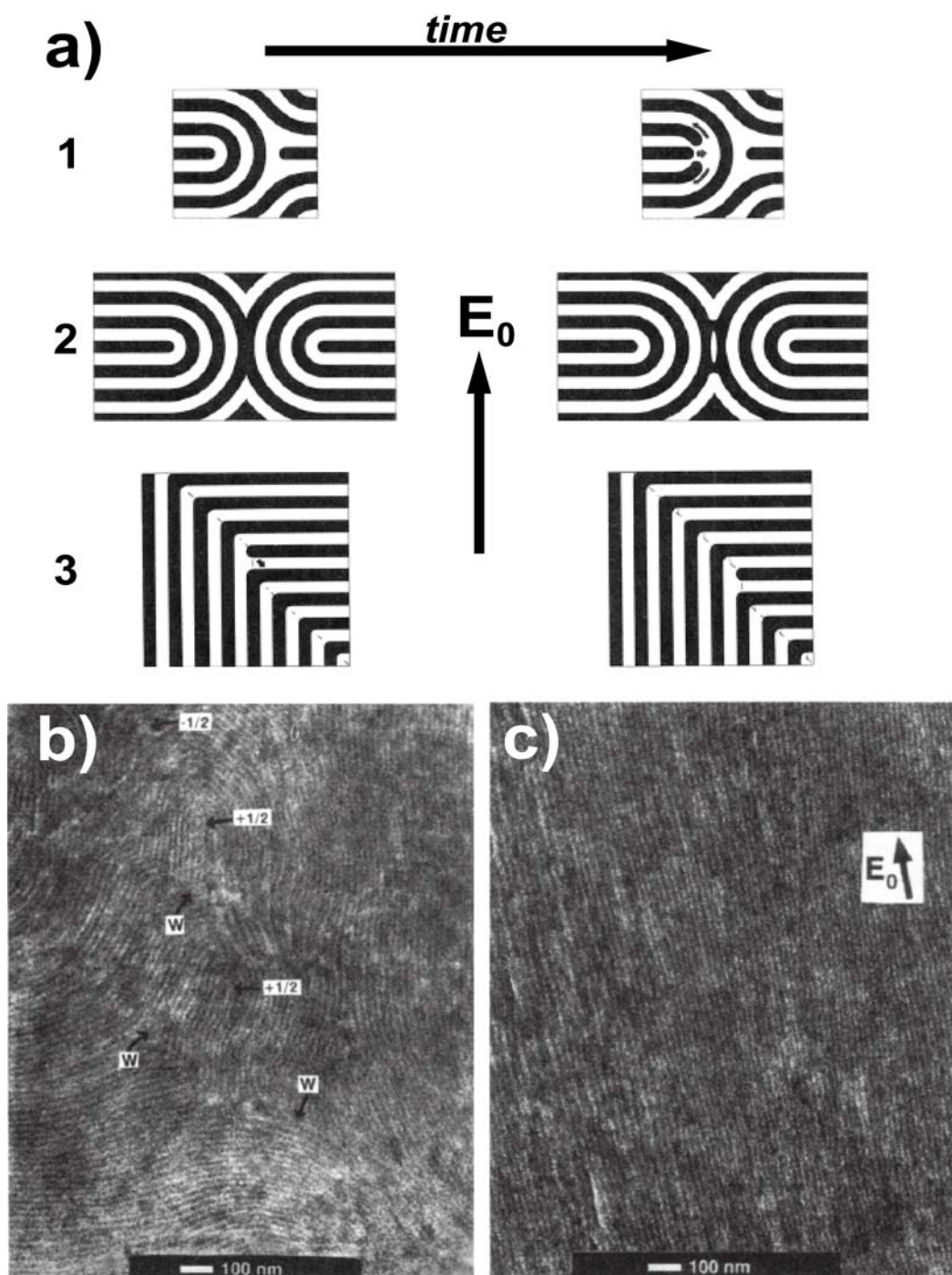


FIGURE 10



Bockstaller et al.

FIGURE 11

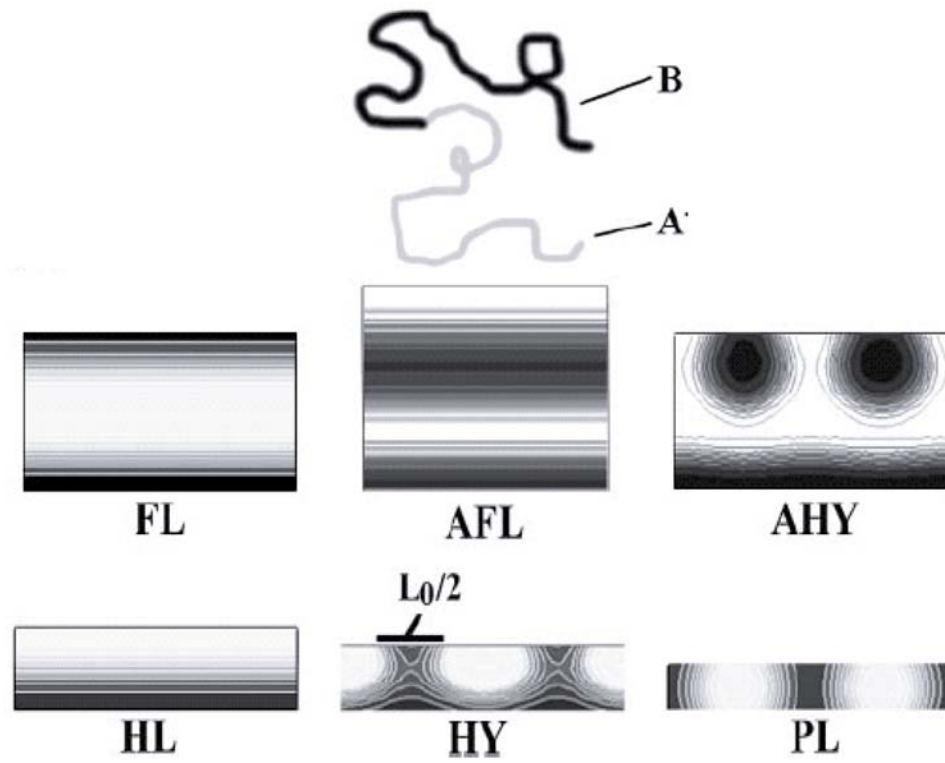
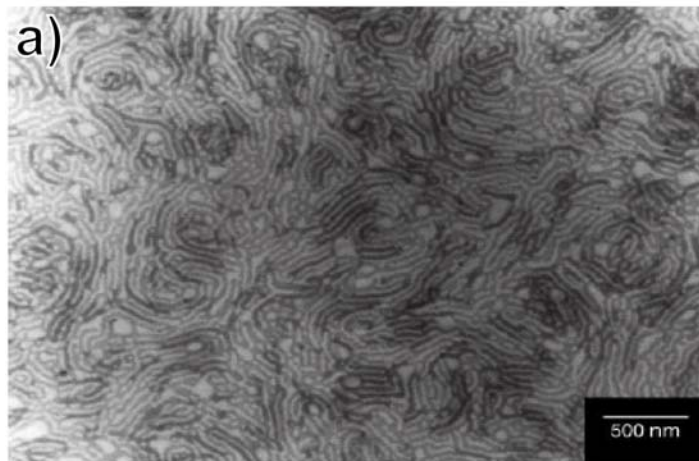
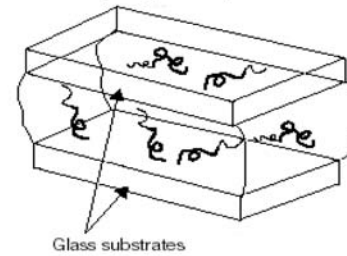


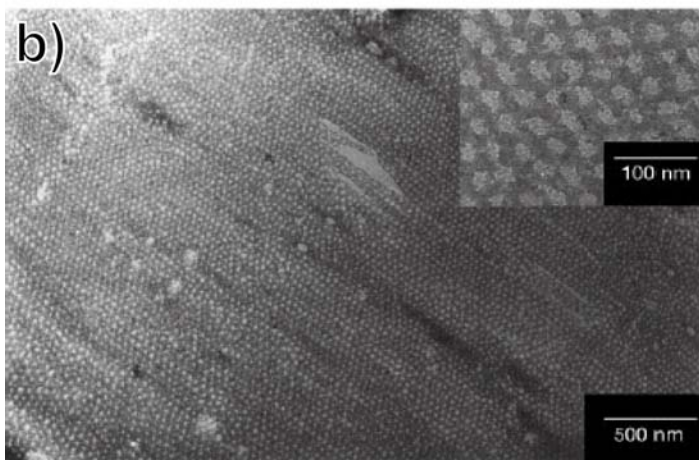
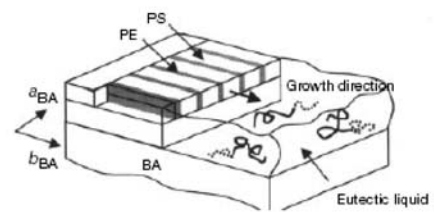
FIGURE 12



**homogeneous mixture
(block copolymer, benzoic acid)**



directional eutectic solidification



**oriented cylinder formation
and epitaxial crystallization**

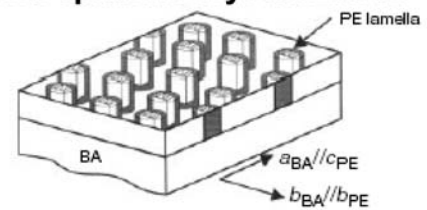
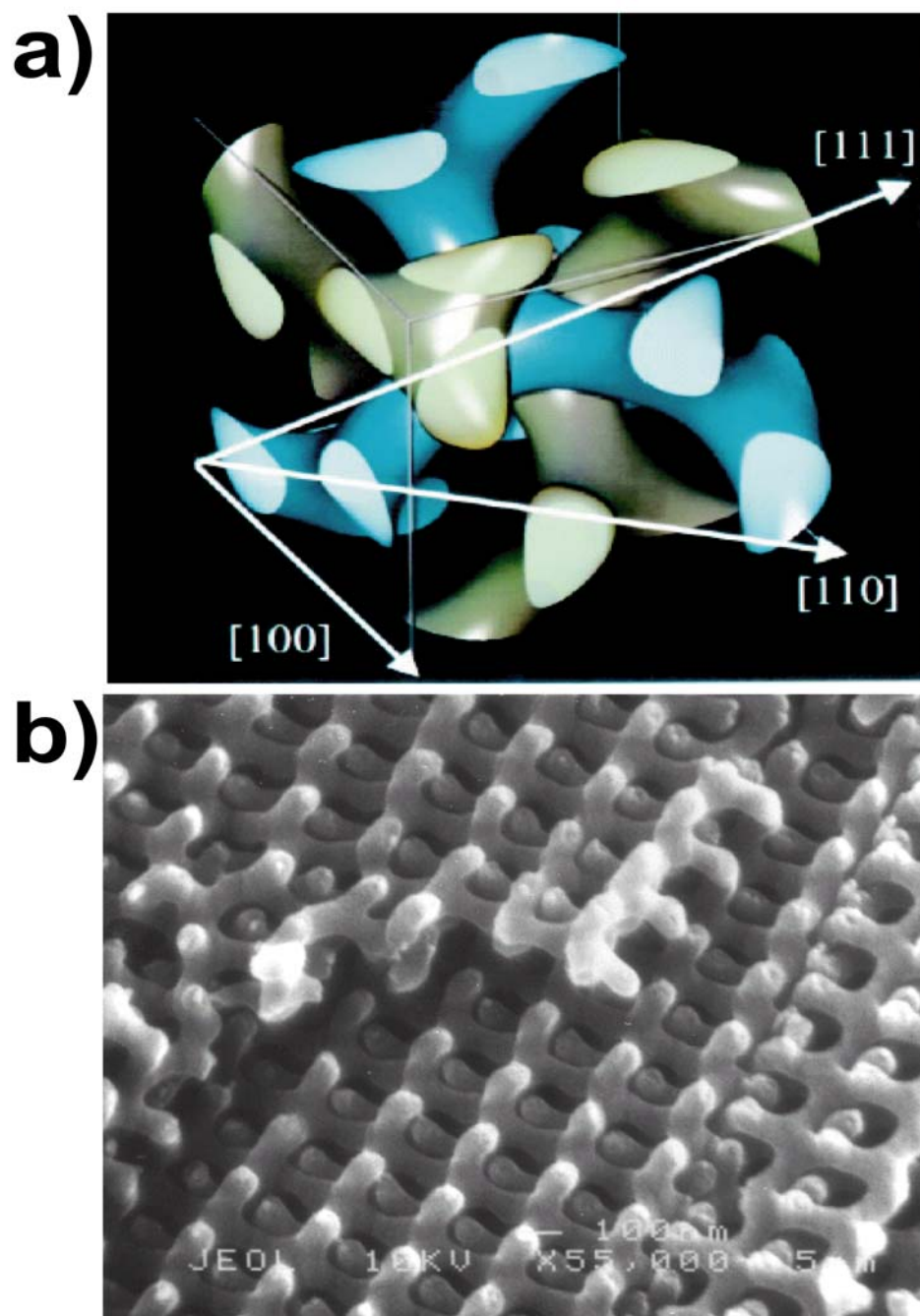
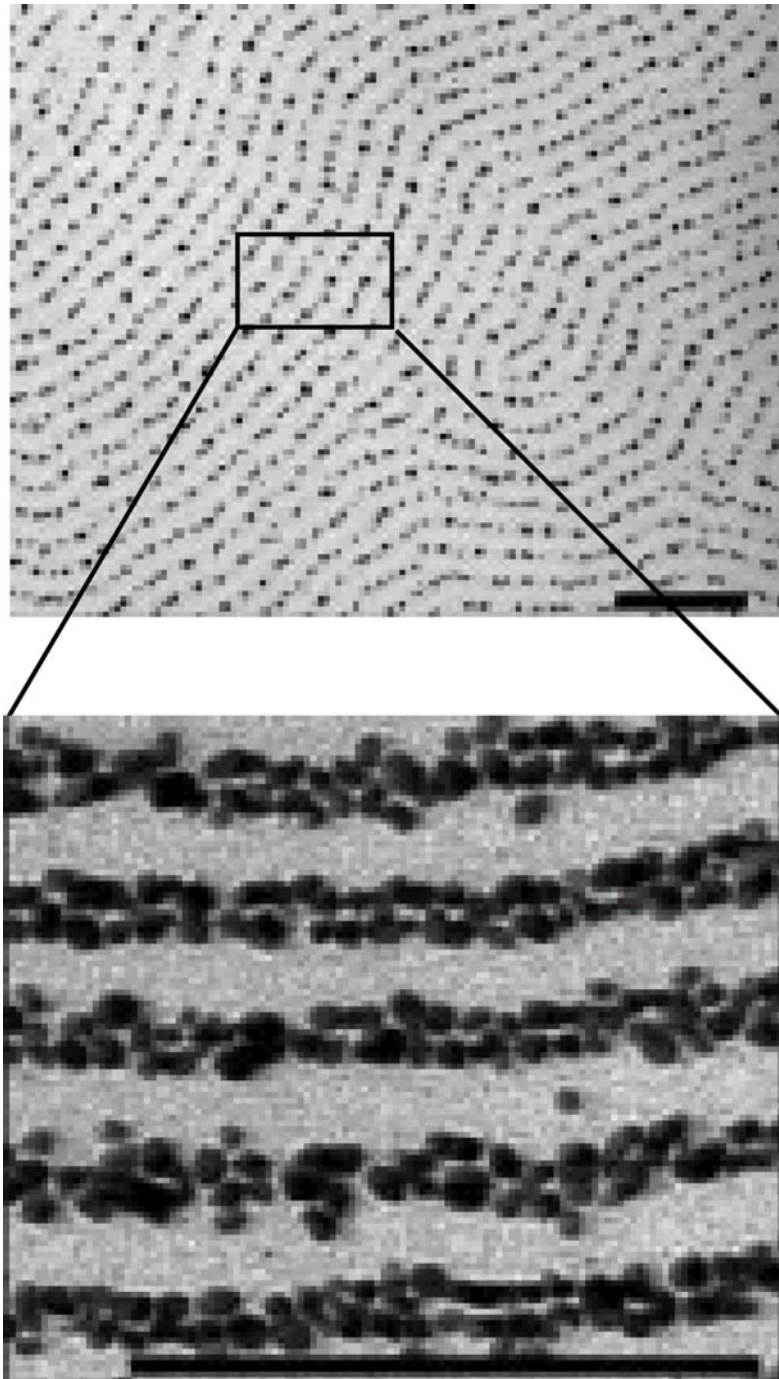


FIGURE 13



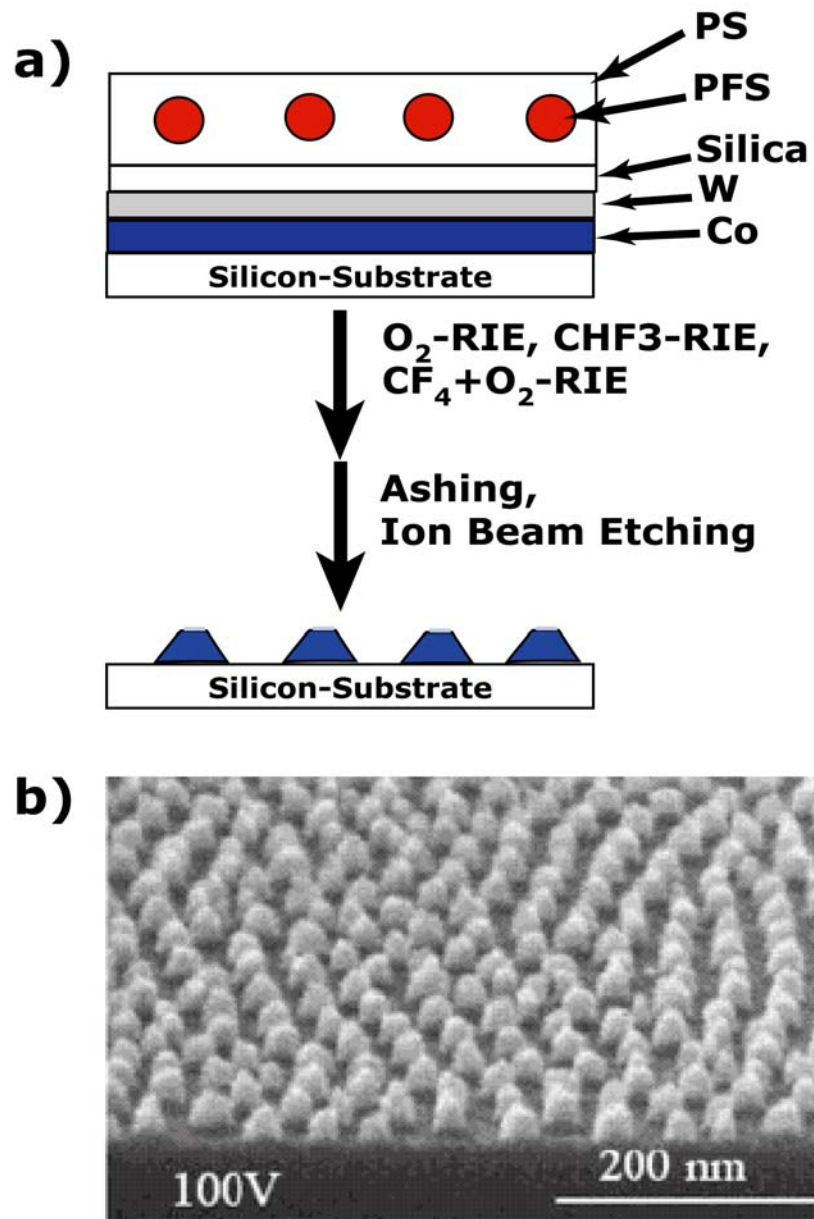
Bockstaller et al.

FIGURE 14



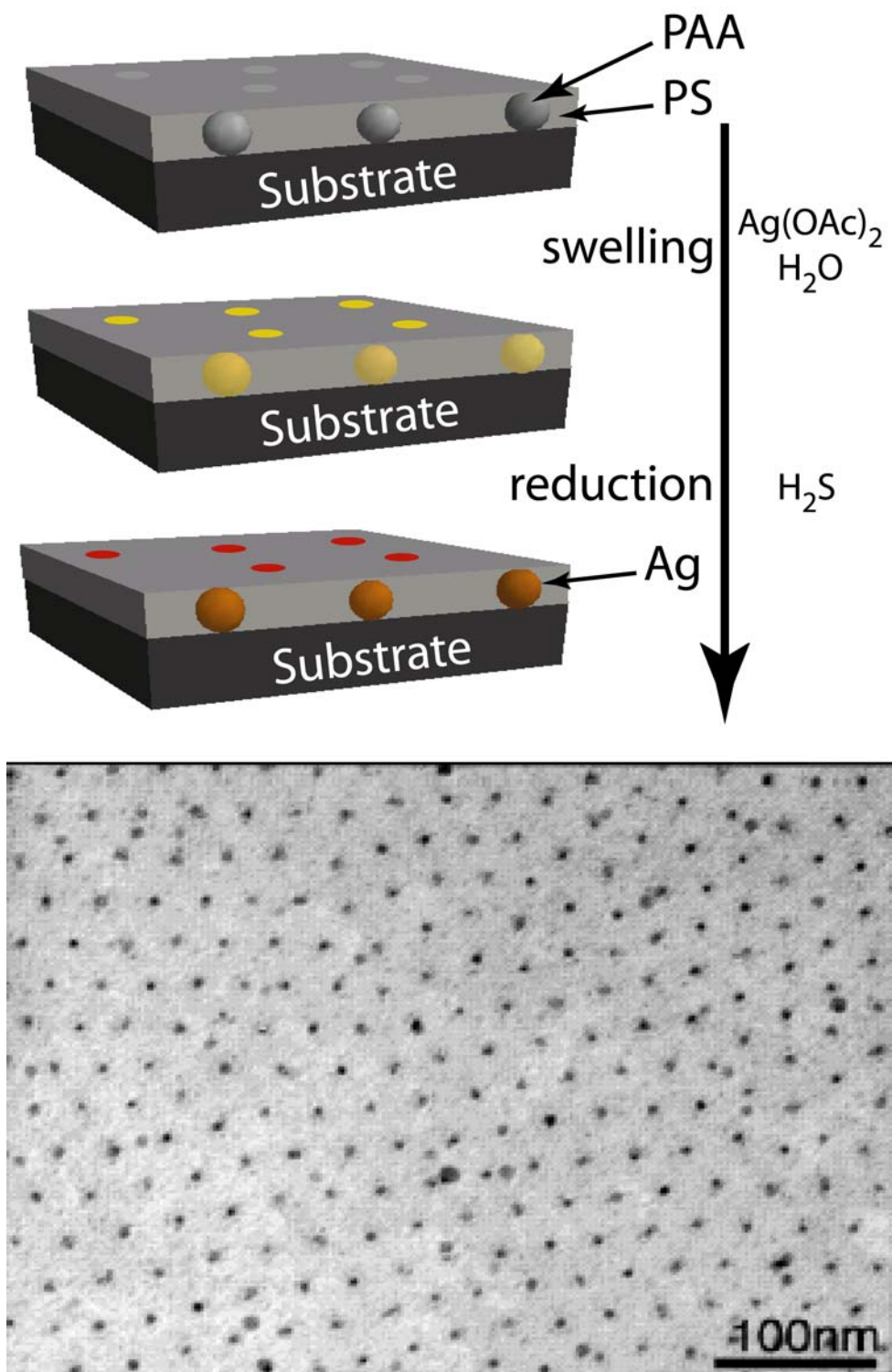
Bockstaller et al.

FIGURE 15



Bockstaller et al.

FIGURE 16



Bockstaller et al.

FIGURE 17

